Title External α carbonic anhydrase and solute carrier 4 (SLC4) bicarbonate transporter are required for HCO_3^- uptake in a freshwater angiosperm

Authors

Wenmin Huang[1,2], Shijuan Han[1,3], Hongsheng Jiang[1], Shuping Gu[4], Wei Li[1,*], Brigitte Gontero[2,*], Stephen C. Maberly[5,*]

[1] Key Laboratory of Aquatic Botany and Watershed Ecology, Wuhan Botanical Garden, Center of Plant Ecology, Core Botanical Gardens, Chinese Academy of Sciences, Wuhan 430074, China

[2] Aix Marseille Univ CNRS, BIP UMR 7281, IMM, FR 3479, 31 Chemin Joseph Aiguier, 13402 Marseille Cedex 20, France

[3] University of Chinese Academy of Sciences, Beijing 100049, China

[4] Shanghai Sequen Bio-info Studio, Shanghai, 200092, China

[5] Lake Ecosystems Group, UK Centre for Ecology & Hydrology, Lancaster Environment Centre, Library Avenue, Bailrigg, Lancaster LA1 4AP, UK

[*]Correspondence: Wei Li (liwei@wbgcas.cn), Brigitte Gontero (bmeunier@imm.cnrs.fr), Stephen C. Maberly (scm@ceh.ac.uk)

Highlight

Acquisition of HCO_3^- in *Ottelia alismoides*, relies on co-diffusion of CO_2 and HCO_3^- through the boundary-layer, conversion of HCO_3^- to CO_2 at the plasmalemma by αCA-1 and transport by SLC4.

Abstract

The freshwater monocot *Ottelia alismoides* is the only known species to operate three CO_2 concentrating mechanisms (CCMs): constitutive HCO_3^--use and C4 photosynthesis, and facultative Crassulacean acid metabolism, but the mechanism of HCO_3^- use is unknown. We found that the inhibitor of an anion exchange (AE) protein, 4,4'-diisothio-cyanatostilbene-2,2'-disulfonate (DIDS), prevented HCO_3^- use but also had a small effect on CO_2 uptake. An inhibitor of external carbonic anhydrase (CA), acetazolamide (AZ), reduced the affinity for CO_2 uptake but also prevented HCO_3^- use via an effect on the AE protein. Analysis of mRNA transcripts identified a homologue of solute carrier 4 (SLC4) responsible for HCO_3^- transport, likely to be the target of DIDS, and a periplasmic αCA-1. We produced a model to quantify the contribution of the three different pathways involved in inorganic carbon uptake. Passive CO_2 diffusion dominates inorganic carbon uptake at high CO_2 concentrations. However, as CO_2 concentrations fall, two other pathways become predominant: conversion of HCO_3^- to CO_2 at the plasmalemma by αCA-1 and, transport of HCO_3^- across the plasmalemma by SLC4. These mechanisms allow access to a much larger proportion of the inorganic carbon pool and continued photosynthesis during periods of strong carbon depletion in productive ecosystems.

Keywords

anion exchanger, bicarbonate, carbonic anhydrase (CA), CO_2 concentrating mechanisms (CCMs), inorganic carbon acquisition, *Ottelia alismoides*, pH drift, photosynthesis, solute carrier 4 (SLC4)

Introduction

Macrophytes form the base of the freshwater food web and are major contributors to primary production, especially in shallow systems (Silva *et al*., 2013; Maberly and Gontero, 2018). However, the supply of CO_2 for photosynthesis in water is potentially limited by the approximately 10,000 lower rate of diffusion compared to that in air (Raven, 1970). This imposes a large external transport resistance through the boundary layer (Black *et al*., 1981), that results in the $K_{½}$ for CO_2 uptake by macrophytes to be 100-200 μM, roughly 6-11 times air-equilibrium concentrations (Maberly and Madsen, 1998). Furthermore, in productive systems the concentration of CO_2 can be depleted close to zero (Maberly and Gontero, 2017). Freshwater plants have evolved diverse strategies to minimize inorganic carbon (Ci) limitation (Klavsen *et al*., 2011) including the active concentration of CO_2 at the active site of ribulose-1,5-bisphosphate carboxylase/oxygenase (Rubisco), collectively known as CO_2 concentrating mechanisms (CCMs). The most frequent CCM in freshwater plants is based on the biophysical uptake of bicarbonate (HCO_3^-), which is present in ~50% of the species tested (Maberly and Gontero, 2017; Iversen *et al*., 2019). While CO_2 can diffuse through the cell membrane passively, HCO_3^- use requires active transport because the plasmalemma is impermeable to HCO_3^- and the negative internal membrane potential (Denny and Weeks, 1970) produces a large electrochemical gradient resisting passive HCO_3^- entry (Maberly and Gontero, 2018).

Detailed studies of the mechanisms of HCO_3^- use have been carried out in microalgae, marine macroalgae, seagrasses and to a lesser extent, freshwater macrophytes (Giordano *et al*., 2005). Direct uptake/transport of HCO_3^- can occur via an anion exchanger (AE) located at the plasmalemma (Sharkia *et al*., 1994). Inhibition of this protein by the membrane impermeable and highly specific chemical, 4,4'-diisothiocyanatostilbene-2,2'-disulfonate (DIDS), has confirmed its effect in a range of marine macroalgae and seagrasses (Drechsler *et al*., 1993; Björk *et al*., 1997; Fernández *et al*., 2014). Genomic studies have found probable AE proteins, from the solute carrier 4 (SLC4) family bicarbonate transporters (Romero *et al*., 2013), in marine microalgae (Nakajima *et al*., 2013; Poliner *et al*., 2015).

Carbonic anhydrase (CA) is a ubiquitous enzyme and is present in photosynthetic organisms. It interconverts CO_2 and HCO_3^-, maintaining equilibrium concentrations when rates of carbon transformation are high (Moroney *et al*., 2001; Dimario *et al*.,

2018). External carbonic anhydrase (CA_{ext}) is inhibited by the impermeable inhibitor acetazolamide (AZ). The widespread nature of CA_{ext} is demonstrated by the inhibition of rates of photosynthesis in a range of aquatic photoautotrophs (James and Larkum, 1996; Larsson and Axelsson, 1999; Moroney *et al*., 2011; Tachibana *et al*., 2011; van Hille *et al*., 2014; Fernández *et al*., 2018). In many marine species, both CA_{ext} and an AE protein are implicated in the uptake of HCO_3^- but very little is known about freshwater macrophytes (Millhouse and Strother, 1986; Beer and Rehnberg, 1997; Björk *et al*., 1997; Gravot *et al*., 2010; Tsuji *et al*., 2017).

Ottelia alismoides (L.) Pers., a member of the monocot family Hydrocharitaceae, possesses two biochemical CCMs: constitutive C4 photosynthesis and facultative Crassulacean Acid Metabolism (CAM; Zhang *et al*., 2014; Shao *et al*., 2017; Huang *et al*., 2018). The leaves of *O. alismoides* comprise epidermal and mesophyll cells that contain chloroplasts and large air spaces but lack Kranz anatomy (Han *et al*., 2020). Although it is known that it can use HCO_3^- in addition to CO_2, little is known about the mechanisms responsible for HCO_3^- uptake. We have addressed this issue, with Ci uptake measurements using the pH-drift technique, experiments with inhibitors of CA and AE and analysis of transcriptomic data.

Materials and methods

Plant material and growth conditions

O. alismoides seeds were sown in soil from Donghu Lake, adjacent to the laboratory in Wuhan, and covered with sterile tap water with an alkalinity of about 2.2 mequiv L^{-1} as described (Huang *et al*., 2018). After a month, seedlings were placed in a 400-L tank (64 cm deep) receiving natural daylight in a glasshouse on the flat roof of the laboratory. The tap water in the tank was changed weekly and snails were removed daily. After nearly two months, the plants in the tank had produced many mature leaves. pH and temperature were measured every day with a combination pH electrode (E-201F, Shanghai Electronics Science Instrument Co., China) connected to a Thermo Orion Dual Star Benchtop pH/ISE Meter. The alkalinity was measured by Gran titration with a standard solution of HCl. CO_2 concentrations were calculated from pH, alkalinity, and temperature using the equations in Maberly (1996). Because of their high biomass the plants generated high pH values (8.3-9.7) and low concentrations of CO_2 (0.11-6.15 μM) in the tank. Information of the conditions in the tank is shown in Supplementary

Table S1.

To examine whether HCO_3^- acquisition was affected by carbon limitation, in a separate experiment *O. alismoides* was incubated at high and low CO_2 concentration for 40 days in plastic containers within one of the tanks in the glasshouse as described previously (Zhang *et al*., 2014). The pH in the low CO_2 treatment (LC) ranged from 8.0 to over 9.8 and the CO_2 concentration ranged from 0.1 to 13 μM with a mean of 2.4 μM. For the high CO_2 treatment (HC), CO_2-saturated tap water was added to the buckets twice each day in order to keep the pH between 6.7-6.8, producing CO_2 concentrations between 481-1110 μM with a mean of 720 μM (Supplementary Table S1). These different CO_2 acclimated leaves were used to detect the effect of AZ and DIDS on Ci uptake rate and external CA activity.

pH-drift experiments

The pH-drift technique was used to determine the capacity of *O. alismoides* to utilize HCO_3^-, and the effects of inhibitors (AZ and DIDS) on photosynthetic Ci uptake (Maberly and Spence, 1983). Measurements were made in a glass and plastic chamber (Maberly, 1990) containing 121 mL of 1 mM HCO_3^- comprising equimolar concentration of $NaHCO_3$ and $KHCO_3$, a pH electrode (model IP-600-9 Jenco Instruments, USA) and an oxygen electrode (Unisense OX-13298). The chamber was placed in a water bath maintained at 25 ℃ and illuminated from the side by fluorescent tubes that provided 75 μmol photon m^{-2} s^{-1} (400-700 nm, Li-Cor sensor connected to a Li-Cor LI-1400 data logger). Prior to the start of the pH drift experiments, the leaves were collected from the tank in the glasshouse in the morning to avoid possible physiological differences caused by a light:dark rhythm of the plant, and then pieces of ~1.1 g fresh weight (FW) of leaf tissue were cut and rinsed in the medium placed in a constant temperature room at 25 ± 2 °C for around 1-4 hours before use. The medium in the incubation chamber was initially bubbled with N_2 to reduce O_2 concentration ~100 ± 20 μM, which was detected by the oxygen electrode connected to an Unisense microsensor multimeter (Version 2.01) and recorded on a laptop computer. At the start of all drift experiments, the pH of the medium was set to 7.6 with CO_2-bubbled medium, and the subsequent changes were measured with the pH electrode connected to a pH meter (model 6311, Jenco Instruments, USA), and recorded on a monitor (TP-LINK, TL-IPC42A-4). The pH-drifts, undertaken at least in triplicate, took 6-23 h to reach an end point value (final pH), which was deemed to be achieved when the pH changed less

than 0.01 unit in one hour (Maberly, 1990). After each drift, the dry weight of the plant material and the alkalinity of the medium were measured, allowing Ci concentrations and Ci uptake rates to be calculated (Maberly and Spence, 1983). When photosynthetic Ci uptake rates were plotted against the total carbon concentration (C_T) at which the rate occurred, a two-phased response curve was observed. The linear response at higher C_T concentration was the consequence of CO_2 use, and the extrapolated intercept with the C_T axis corresponded to the CO_2 compensation point (Maberly and Spence, 1983).

Effect of inhibitors on Ci-uptake and external CA activity

Inhibitors were used in pH-drift experiments to determine their effect on Ci-uptake. A stock solution of AZ (20 mM) was prepared by dissolving the solid in 20 mM NaOH and 0.61 or 1.21 mL was injected into the chamber to produce final concentration of 0.1 or 0.2 mM respectively. Stock solutions of 30 mM DIDS, were prepared daily by dissolving the powder in distilled water (Cabantchik and Greger, 1992), and 1.21 mL was injected into the chamber to produce a final concentration of 0.3 mM. Both stock solutions were kept in the dark at 4°C.

To check if the inhibitory effect of AZ on HCO_3^- uptake was reversible, we performed three consecutive drifts using the same *O. alismoides* leaf cut longitudinally into two halves. The first half was used as a control (first drift) without AZ. The second half was treated with AZ (second drift). Subsequently, this leaf and chamber were thoroughly rinsed with clean medium three times over ten minutes, and finally a post-control (third drift), was performed without the inhibitor. All the pH-drifts were started at pH 7.6 and stopped at pH 8.5 and replicated at least in triplicate.

External CA activity

The CA_{ext} activity was measured as in Fernández *et al*. (2018) with small modifications, using commercial CA (Sigma, C4396) as a positive control and to check activity linearity (Supplementary Fig. S1). A 50 mL plastic tube was placed inside a container filled with ice that maintained the temperature at 0-4°C. Approximately 60 mg FW leaf was placed in the tube containing 10 mL of buffer (pH 8.5): 50 mM Tris, 2 mM DTT, 15 mM ascorbic acid, 5 mM Na_2-EDTA and 0.3% w/v polyvinylpyrrolidone (PVP). Temperature and pH were simultaneously measured using a pH meter. The reaction was started by rapidly introducing 5 mL of ice-cold CO_2 saturated water and pH was recorded over time. The relative enzyme activity (REA) was determined using the

equation below:

$$REA = (T_b/T_s)-1 \quad (1)$$

where T_b and T_s are the times in seconds required for the pH to drop from pH 8.3 to 7.9 in the non-catalyzed (without sample) and catalyzed reactions, respectively. The REA was expressed on a fresh weight basis. In the leaves grown at LC and HC, external CA activity was measured in the presence of 0.1 mM and 0.2 mM AZ as well as 0.3 mM DIDS.

Transcriptomic analysis

CA_{ext} and AE proteins were searched for within a transcriptome dataset obtained from *O. alismoides* acclimated to LC and HC (Huang *et al*., 2018). Information of the different CO_2 treatments is shown in Supplementary Table S1. Six samples (three HC and three LC acclimated mature leaves) were used for second-generation sequencing (SGS) for short but high-accuracy reads (Hackl *et al*., 2014). Six other samples were used for the third-generation sequencing (TGS) for longer sequences but lower-quality reads (Roberts *et al*., 2013).

Around 0.3 g fresh weight leaves were collected 30 minutes before the end of the photoperiod, flash frozen in liquid N_2 and stored at -80°C before use. Total RNA was extracted using a commercial kit RNAiso (Takara Biotechnology, Dalian, China). The purified RNA was dissolved in RNase-free water, with genomic DNA contamination removed using TURBO DNase I (Promega, Beijing, China). RNA quality was checked with the Agilent 2100 Bioanalyzer (Agilent Technologies, Palo Alto, California). Only the total RNA samples with RNA integrity numbers ≥8 were used to construct the cDNA libraries in PacBio or Illumina Hiseq sequencing.

For TGS analysis, total RNA (2 μg) was reversely transcribed into cDNA using the SMARTer PCR cDNA Synthesis Kit that has been optimized for preparing high-quality, full-length cDNAs (Takara Biotechnology, Dalian, China), followed by size fractionation using the BluePippin™ Size Selection System (Sage Science, Beverly, MA). Each SMRT bell library was constructed using 1-2 μg size-selected cDNA with the Pacific Biosciences DNA Template Prep Kit 2.0. SMRT sequencing was then performed on the Pacific Bioscience sequel platform using the manufacturer's protocol.

For SGS analysis, cDNA libraries were constructed using a NEBNext® Ultra™ RNA Library Prep Kit for Illumina® (NEB, Beverly, MA, USA), following the manufacturer's protocol. Qualified libraries were sequenced, and 150 bp paired-end

reads were generated (Illumina Hiseq 2500, San Diego, CA, USA).

The TGS subreads were filtered using the standard protocols in the SMRT analysis software suite (http://www.pacificbiosciences.com) and reads of insert (ROIs) were generated. Full-length non-chimeric reads (FLNC) and non-full-length cDNA reads (NFL) were recognized through the identification of poly(A) signal and 5' and 3' adaptors. The FLNC reads were clustered and polished by the Quiver program with the assistance of NFL reads, producing high-quality isoforms (HQ) and low-quality isoforms (LQ). The raw Illumina reads were filtered to remove ambiguous reads with 'N' bases, adaptor sequences and low-quality reads. Filtered Illumina data were then used to polish the LQ reads using the proovread 213.841 software. The redundant isoforms were then removed to generate a high-quality transcript dataset for *O. alismoides*, using the program CD-HIT.

TransDecoder v2.0.1 (https://transdecoder.github.io/) was used to define the putative coding sequence (CDS) of these transcripts. The predicted CDS were then functional annotated and confirmed by BLAST, which was conducted against the following databases: NR, NT, KOG, COG, KEGG, Swissprot and GO. For each transcript in each database searched, the functional information of the best matched sequence was assigned to the query transcript. The phylogenetic tree of αCA-1 isoforms based on deduced CA peptide sequences from the NCBI, was analyzed with Geneious software (Windows version 11.0, Biomatters Ltd, New Zealand). The location of the protein was analyzed using Target P1 (Emanuelsson *et al.*, 2007; http://www.cbs.dtu.dk/services/TargetP/).

Statistical analysis

All data presented in this study are the mean ±SD. Mean final pH values were calculated geometrically. One-way ANOVA was used to test for significant variation, after homogeneity and normality were satisfied. Duncan's and Tukey's post-hoc tests were used to test for significance among treatments while percentage data were compared using a non-parametric Mann–Whitney test. The threshold of statistical significance was set at $P<0.05$. The data were analyzed using SPSS 16.0 (SPSS Inc., Chicago, IL, USA).

Results

In control leaves, the pH drift end point was reached after nearly 24 hours at a mean pH

of 10.2 (Fig. 1, 2A) and a very low final CO_2 concentration of ~0.03 µM (about 450-fold below air equilibrium, and at an oxygen concentration of about 353 µM, about 137% of air-equilibrium; Fig. 2B) indicating that HCO_3^- had been used. In leaves treated with AZ or DIDS, the pH drift stopped after 6 to 12 hours and the end point did not exceed pH 9.3; final CO_2 concentrations were between 0.8 and 1.6 µM (Fig. 1, Fig. 2A, 2B), indicating that HCO_3^- use had been inhibited. As a consequence of HCO_3^- use in control leaves, rates of Ci uptake were about 40 µmol g^{-1} DW h^{-1} even at the very low CO_2 concentrations (Supplementary Fig. S2). The slope of Ci uptake *vs* concentration of CO_2 between 15 and 40 µM in leaves treated with AZ was between 54.1% and 70.6% lower than the control ($P<0.05$) and in leaves treated with DIDS, it was about 35% lower than the control ($P<0.05$; Fig. 2C). In contrast, the intercept CO_2 compensation points increased significantly as a result of the addition of AZ (Fig. 2D). The higher AZ concentration treatments had a CO_2 compensation concentration close to 20 µM (at an oxygen concentration of 163 µM) suggesting that CCM is absent. These results suggest that AZ not only inhibited CA_{ext} but also inhibited the AE protein. The CO_2 compensation concentration in the presence of DIDS, at about 5 µM (at an oxygen concentration of 232 µM, about 90% of air-equilibrium), was not significantly different from the control but substantially lower than in the two AZ treatments (Fig. 2D). The C_T/alkalinity quotient (the remaining total Ci at the end of the drift, C_T related to the alkalinity) is a measure of the effectiveness of Ci depletion. A low quotient indicates that a large proportion of the Ci pool is available for acquisition and vice versa. While HCO_3^- use in control leaves allowed about half of the available inorganic carbon to be accessible, in the AZ and DIDS treated leaves, a high quotient was obtained and only between 11 and 16% of the available inorganic carbon was accessible (Fig. 2E).

Fig. 3 shows the Ci uptake rates at different CO_2 concentrations calculated from the pH-drift experiments over a pH range from about 7.7 to 9.3. AZ inhibited Ci-uptake at all the CO_2 concentrations (Fig. 3A), and both AZ concentrations inhibited Ci uptake by between 70 and 76% when the concentrations of CO_2 were between 2.6 and 11 µM. In contrast, DIDS did not affect Ci uptake at CO_2 concentrations above 4.2 µM but inhibited Ci uptake by about 40% at CO_2 concentrations between about 1 and 4 µM

(Fig. 3B). The inhibitory effect caused by AZ at both concentrations, can be completely reversed by washing since the post-control rates of Ci uptake were not significantly different from the initial control ($P>0.05$; Fig. 4). This confirms that AZ does not penetrate the plasmalemma (Moroney *et al*., 1985) and thus that the observed effects are linked to inhibition of CA_{ext}.

The inhibition of Ci uptake rates in the presence of 0.1 mM AZ and 0.3 mM DIDS were not significantly different in leaves acclimated to HC *vs* LC, although there was a slightly greater inhibition by 0.2 mM AZ in HC compared to LC leaves ($P<0.05$; Fig. 5A, 5B). CA_{ext} activity was present in both HC and LC leaves but it was greater in LC leaves ($P<0.01$; Fig. 5C). CA_{ext} activity was inhibited by AZ: the 0.2 mM treatment caused a greater inhibition than 0.1 mM AZ (Fig. 5D). DIDS had no effect on CA_{ext} activity neither in HC nor in LC leaves. Ci uptake rates, measured at an initial CO_2 concentration of 12 µM, were broadly positively related to the activity of CA_{ext} (R^2 = 0.84 and 0.74 for HC and LC leaves respectively, $P<0.01$).

The inhibition of Ci uptake in *O. alismoides* by AZ and DIDS implied that both CA_{ext} and anion exchange protein were present. This was characterized further using transcriptomic analysis: mRNA for putative alpha carbonic anhydrase 1 (αCA-1) and HCO_3^- transporters were expressed. Fifty-three transcripts were functionally annotated to CA according to sequence similarity and translated into 66 peptides. Six of these peptides were homologous with αCA1 based on a comparison of amino acid sequences with the NCBI database and corresponded to four CA isoforms (Fig. 6A, Supplementary Fig. S3). Isoform 1 in *O. alismoides* shows 60% and 61% identity with the chloroplastic isoform X1 and X2 of αCA-1 from the monocot *Musa acuminata*. Isoforms 2, 3 and 4 show 58%, 55% and 56% identity with the isoform X1 from this species, respectively, as well as 59%, 57% and 58% identity with the isoform X2. However, according to Target P1 software, all the isoforms from *O. alismoides* were predicted to be localized in the secretory pathway (Fig. 6B). The expression of the four isoforms of putative αCA-1, was not significantly different in HC and LC acclimated leaves ($P>0.05$, Fig. 6C).

Unfortunately, transcripts of HCO_3^- transporters were not detected due to the lower sensitivity of TGS, but were present in the dataset from SGS. Fifteen peptides sequences (Supplementary Fig. S3) were inferred to be homologous to HCO_3^- transporter family with the following dicot species in the database: *Artemisia annua*

(70.6-78.9%), *Corchorus olitorius* (73.1-85.7%), *Corchorus capsularis* (73.1-85.7%), *Cynara cardunculus* (80.4-85.7%), *Lupinus albus* (73.22%), *Macleaya cordata* (76.2-83.5%), *Parasponia andersonii* (74.0%), *Populus alba* (77.6%), *Prunus dulcis* (78.5-82.4%), *Striga asiatica* (81.6-83.5%), *Theobroma cacao* (79.2-85.0%) and *Trema orientale* (75.1-75.8%). This HCO_3^- transporter family contains Band 3 anion exchange proteins, which also known as anion exchanger 1 or SLC4 member 1. Only partial sequences could be deduced from our analysis and since the peptides for putative HCO_3^- transporters are membrane proteins, their location could not be predicted. The mRNA expressions of all the transcripts for putative SLC4 HCO_3^- transporters were not significantly different in HC and LC acclimated leaves ($P>0.05$, data not shown); the expression-data for the highest expressed transcript for SLC4 HCO_3^- transporters is presented in Fig. 6D.

Discussion

O. alismoides possesses three CCMs, including constitutive abilities to (i) use HCO_3^- and (ii) operate C4 photosynthesis, and a facultative ability to perform CAM when acclimated to low CO_2 concentrations (Zhang *et al*., 2014; Shao *et al*., 2017; Huang *et al*., 2018). We confirm here that this species has a constitutive ability to use HCO_3^-, and this allows it to exploit a large proportion of the Ci pool and drive CO_2 to very low concentrations.

In this study, multiple lines of evidence show that an external CA, putative αCA-1, plays a major role in Ci uptake in *O. alismoides*: (i) external CA activity was measured, (ii) AZ inhibited Ci uptake with the slope of Ci uptake *vs* the concentration of CO_2 between 15 and 40 μM being about a quarter of the control after treatment with 0.2 mM AZ, (iii) transcripts of putative αCA-1 were detected. The CA was confirmed to be external since (i) washing of leaves treated with AZ, restored CA activity and (ii) its sequence bears a signal peptide consistent with a periplasmic location. External CA is indeed widespread in photoautotrophs from marine and freshwater environments (Moroney *et al*., 2001; Dimario *et al*., 2018). The green microalga *Chlamydomonas reinhardtii* has three αCAs, of which two (Cah1 and Cah2) are localized in the periplasmic space and one (Cah3) in the thylakoid membrane (Fujiwara *et al*., 1990; Karlsson *et al*., 1998; Moroney and Chen, 1998). While CAs have the same catalytic activity, their sequence identity could be very low among different classes (Jensen *et*

al., 2019). The αCA-1 from *O. alismoides* has around 30% sequence identity with the periplasmic Cah1 from *C. reinhardtii*. Many CAs are regulated by the concentration of CO_2. The diatom *Phaeodactylum tricornutum* does not possess external CA, but the internal CA (β-type CA) is CO_2 responsive and crucial for its CCM operation (Satoh *et al*., 2001; Harada *et al*., 2005; Harada and Matsuda, 2005; Tsuji *et al*., 2017). In the marine diatom, *Thalassiosira pseudonana*, the two external CAs, δ-CA and ζ-CA, as well as a recently identified chloroplastic ι-CA are induced by carbon limitation (Samukawa *et al*., 2014; Clement *et al*., 2017; Jensen *et al*., 2019). In contrast, the putative αCA-1 in *O. alismoides* is constitutive and its expression was unaffected by the CO_2 concentration. This is also true for Cah3 in the thylakoid lumen of *C. reinhardtii* (Karlsson *et al*., 1998; Moroney and Chen, 1998), while the expression of the periplasmic CA (Cah1) and the mitochondrial CAs (β-CA1 and β-CA2) are highly CO_2-sensitive (Moroney and Chen, 1998).

We show that the anion exchange proteins, one group of the SLC4 family HCO_3^- transporters (Romero *et al*., 2013), is involved in HCO_3^- uptake in *O. alismoides*. DIDS, a commonly-used inhibitor of AE/SLC-type HCO_3^- transporters (Romero *et al*., 2013) significantly decreased the final pH of a drift, and increased the final CO_2 concentration to about 0.8 μM which is not substantially less than that expected in the absence of a CCM: a terrestrial C_3 plant CO_2 compensation point of 36 μL L^{-1} (Bauer and Martha, 1981) is equivalent to about 1.2 μM. Furthermore, transcripts of putative HCO_3^- transporter family in *O. alismoides* were found to contain Band 3 anion exchange proteins (SLC4 member 1), and the peptides shared 70.6-85.7% sequence identity with HCO_3^- transporters from other terrestrial plant species. Several genes which encode SLC4 family transporters, has been found to be involved in the CCMs in the marine microalgae *Phaeodactylum tricornutum and Nannochloropsis oceanica* (Nakajima *et al*., 2013; Poliner *et al*., 2015), as well as the marine macroalga *Ectocarpus siliculosus* (Gravot *et al*., 2010). More broad evidence from the physiological data have demonstrated that anion exchange proteins play a role in HCO_3^- uptake in green, red and brown marine macroalgae (Drechsler *et al*., 1993; Granbom and Pedersén, 1999; Larsson and Axelsson, 1999; Fernández *et al*., 2014). Although HCO_3^- use by seagrasses is known to involve an anion exchange protein, to our knowledge, this is the first report that provides evidence of the presence of a direct HCO_3^- uptake via DIDS-sensitive SLC4 HCO_3^- transporters in an aquatic angiosperm. Whatever, these

transporters for direct HCO_3^- acquisition, appears to be much more restricted in distribution than the widespread external CA.

Three mechanisms of HCO_3^- use have been proposed in aquatic plants: i) indirect use of HCO_3^- based on dehydration of HCO_3^-, facilitated by external CA, to produce elevated CO_2 concentrations outside the plasmalemma; ii) direct uptake of HCO_3^- by an anion exchange transporter in the plasmalemma and iii) direct uptake of HCO_3^- by a P-type H^+-ATPase (Giordano *et al*., 2005). In this study we provide evidence for the first two mechanisms in *O. alismoides*. Although we did not specifically check for a P-type H^+-ATPase, this process appears to be absent, or of minor importance, in *O. alismoides* in contrast to *Laminaria digitata* and *L. saccharina* (Klenell *et al*., 2004), because in *O. alismoides,* HCO_3^- use was abolished by addition of either AZ or DIDS. An AE is mainly responsible for HCO_3^- use in the brown marine macroalga *Macrocystis pyrifera* (Fernández *et al*., 2014), while in several other brown macroalgae such as *Saccharina latissima* (formerly *Laminaria saccharina*) external CA plays the major role in HCO_3^- use (Axelsson *et al*., 2000), though in *L. saccharina* as in *L. digitate*, a P-type H^+-ATPase has been identified (Klenell *et al*., 2004). In another brown macroalga, *Endarachne binghamiae*, HCO_3^- use was based on an external CA and P-type H^+-ATPase with no contribution from an AE (Zhou and Gao, 2010). Another strategy to use HCO_3^- has been shown in some species of freshwater macrophytes that involves the possession of 'polar leaves' (Steemann-Nielsen, 1947). At the lower surface of these leaves, proton extrusion generates low pH and at their upper surface, high pH often generates calcite precipitation (Prins *et al*., 1980). Consequently, at the lower surface with low pH, the conversion of HCO_3^- to CO_2 near the plasmalemma facilitates the cells to take up Ci. Because of this, there is some evidence for a lower reliance on external CA in macrophytes with polar leaves. For example, in a species with polar leaves, *Potamogeton lucens*, external CA was absent (Staal *et al*., 1989) and in the polar leaf species *Elodea canadensis*, external CA activity was present but not influenced by the CO_2 concentration (Elzenga and Prins, 1988).

It was initially surprising that AZ completely inhibited HCO_3^- use. However, Sterling *et al*. (2001) also found that AZ inhibited AE1-mediated chloride-bicarbonate exchange. This result could be explained by the binding of CA to the AE resulting in the formation of a transport metabolon, where there was a direct transfer of HCO_3^- from CA active site to the HCO_3^- transporter (Sowah and Casey, 2011; Thornell and

Bevensee, 2015). Thus, when CA is inhibited, then the transport of HCO_3^- is inhibited.

O. alismoides can perform C4 photosynthesis, however the final CO_2 concentration at the end of pH-drift, when HCO_3^--use was abolished by the inhibitors, was 0.8-1.6 µM, which could be supported by passive entry of CO_2 without the need to invoke a CCM. These are slightly higher than the CO_2 compensation point in the freshwater C4 macrophyte *Hydrilla verticillata* at less than 10 ppm (Bowes, 2010), which is equivalent to a dissolved CO_2 ~0.3 µM at 25 °C. If this difference between the species is real and not methodological, it could suggest that in *O. alismoides* C4 photosynthesis is more important to suppress photorespiration than to uptake carbon.

A simple model of carbon acquisition (Fig. 7A) was constructed to quantify the contribution of the three pathways involved in Ci uptake in *O. alismoides*: passive diffusion of CO_2, HCO_3^--use involving αCA-1 and HCO_3^--use involving SLC4 HCO_3^- transporters. Using the Ci uptake rates at different CO_2 concentrations in Fig. 3, and assuming that 0.3 mM DIDS completely inhibited HCO_3^- transporters and that 0.2 mM AZ completely inhibited αCA-1 and HCO_3^- transporters, we calculated: i) passive diffusion of CO_2 as the rate in the 0.2 mM AZ treatment that inhibited both αCA-1 and SLC4 HCO_3^- transporters; ii) diffusion of HCO_3^- and conversion to CO_2 by αCA-1 at the plasmalemma as the difference between the rate in the presence of 0.3 mM DIDS and that in the presence of 0.2 mM AZ; and iii) diffusion of HCO_3^- and transfer across the plasmalemma by SLC4 HCO_3^- transporters as the difference in the rate between the control and the 0.3 mM DIDS treatment. At a CO_2 concentration of about 50 µM, passive diffusion of CO_2 contributed 55.7% to total Ci uptake, diffusion of HCO_3^- and conversion to CO_2 by αCA-1 contributed 42.7% and transfer of HCO_3^- across the plasmalemma by SLC4 HCO_3^- transporters contributed 1.6% (Fig. 7B). At ~9 µM (about 66% of equilibrium with air at 400 ppm CO_2) the contribution to total Ci uptake of CO_2-diffusion, HCO_3^- diffusion and conversion to CO_2 by αCA-1 and transfer by SLC4 HCO_3^- transporters was 24.0%, 64.4% and 11.5% respectively and at about 1 µM CO_2 (close to a typical C3 CO_2 compensation point) diffusion was zero and αCA-1 and SLC4 HCO_3^- transporters contributed equally to carbon uptake. So, as CO_2 concentrations fall, passive CO_2 diffusion can no longer support Ci uptake and indirect and direct use of HCO_3^- allows Ci uptake to continue. The stimulation of absolute rates of SLC4 HCO_3^- transporters-dependent Ci uptake is consistent with patterns seen for a number of freshwater macrophytes during pH-drift experiments, where rates increase

as CO_2 approaches zero before declining as Ci is strongly depleted (Maberly and Spence, 1983). This could be caused by regulation or by direct effects of pH on HCO_3^- transporters activity.

These results confirm the prevailing notion from seagrasses that external CA plays an important role in contributing to Ci uptake. External CA contributed 25% to Ci uptake in *Posidonia australis* (James and Larkum, 1996) and ~60% in *Zostera marina* (approximately 2.2 mM Ci at pH 8.2, equivalent to a dissolved CO_2 ~23 μM at 25 °C; Beer and Rehnberg, 1997), albeit in the presence of Tricine buffer that might inhibit the photosynthesis rate. The value reported here for *O. alismoides* at a CO_2 concentration of 23 μM, 56%, is similar to *Z. marina*.

In conclusion, *O. alismoides* has developed a jack of trades CCM, the master of which, either external CA or SLC4 HCO_3^- transporters, depends on the CO_2 concentration. There are several future lines of work that need to be pursued. The distribution of HCO_3^- transporters in freshwater species should be determined. The apparent relationship between polar leaves and low or absent external CA activity could be tested using a range of species, especially within the genus *Ottelia* where calcite precipitation differs among species (Cao *et al*., 2019). The Ci acquisition mechanisms of more freshwater species should be examined. The cause of the increasing rate of HCO_3^- transporters-dependent HCO_3^- uptake as Ci becomes depleted needs to be understood. Finally, production and analysis of genome sequences for freshwater macrophytes will be a powerful tool to answer these and future questions concerning the strategies used by freshwater macrophytes to optimize photosynthesis.

Supplementary data

Fig. S1. Commercial CA was used as a positive control and to check activity linearity.

Fig. S2. The Ci uptake rate *vs* the CO_2 concentration at which that rate occurred in *O. alismoides* treated without (control) or with inhibitors (AZ and DIDS).

Fig. S3. Amino acid sequences of peptides for putative carbonic anhydrase and bicarbonate transporters from *O. alismoides*.

Table S1. Information on the different CO_2 acclimation experiments.

Acknowledgements

468 This work was supported by the Strategic Priority Research Program of the Chinese
469 Academy of Sciences (Grant No. XDB31000000), Chinese Academy of Sciences
470 President's International Fellowship Initiative to SCM and BG (2015VBA023,
471 2016VBA006), and the National Natural Science Foundation of China (Grant No.
472 31970368).

473

References

Axelsson L, Mercado JM, Figueroa FL. 2000. Utilization of HCO_3^- at high pH by the brown macroalga *Laminaria saccharina*. European Journal of Phycology **35,** 53–59.

Bauer H, Martha P. 1981. The CO_2 compensation point of C3 plants-A re-examination I. Interspecific variability. Zeitschrift für Pflanzenphysiologie **103,** 445–450.

Beer S, Rehnberg J. 1997. The acquisition of inorganic carbon by the seagrass *Zostera marina*. Aquatic Botany **56,** 277–283.

Björk M, Weil A, Semesi S, Beer S. 1997. Photosynthetic utilization of inorganic carbon by seagrasses from Zanzibar, East Africa. Marine Biology **129,** 363–366.

Black MA, Maberly SC, Spence DHN. 1981. Resistance to carbon dioxide fixation in four submerged freshwater macrophytes. New Phytologist **89,** 557–568.

Bowes G. 2010. Chapter 5 Single-Cell C4 Photosynthesis in Aquatic Plants. In: Raghavendra A, Sage R. (eds) C4 Photosynthesis and Related CO_2 Concentrating Mechanisms. Advances in Photosynthesis and Respiration **32**, 63–80. Springer, Dordrecht.

Cabantchik ZI, Greger R. 1992. Chemical probes for anion transporters of mammalian cell membranes. American Journal of Physiology **262,** C803–C827.

Cao Y, Liu Y, Ndirangu L, Li W, Xian L, Jiang HS. 2019. The analysis of leaf traits of eight *Ottelia* populations and their potential ecosystem functions in Karst freshwaters in China. Frontiers in Plant Science **9,** 1938.

Clement R, Lignon S, Mansuelle P, Jensen E, Pophillat M, Lebrun R, Denis Y, Puppo C, Maberly SC, Gontero B. 2017. Responses of the marine diatom *Thalassiosira pseudonana* to changes in CO_2 concentration: a proteomic approach. Scientific Reports **7,** 42333.

Denny P, Weeks DC. 1970. Effects of light and bicarbonate on membrane potential in *Potamogeton schweinfurthii* (Benn). Annals of Botany **34,** 483–496.

DiMario RJ, Machingura MC, Waldrop GL, Moroney JV. 2018. The many types of carbonic anhydrases in photosynthetic organisms. Plant Science **268,** 11–17.

Drechsler Z, Sharkia R, Cabantchik ZI, Beer S. 1993. Bicarbonate uptake in the marine macroalga *Ulva* sp. is inhibited by classical probes of anion exchange by red blood cells. Planta **191,** 34–40.

Elzenga JTM, Prins HBA. 1988. Adaptation of *Elodea* and *Potamogeton* to different inorganic carbon levels and the mechanism for photosynthetic bicarbonate utilization. Australian Journal of Plant Physiology **15,** 727–735.

Emanuelsson O, Brunak S, von Heijne G, Nielsen H. 2007. Locating proteins in the cell using TargetP, SignalP and related tools. Nature Protocol **2,** 953–971.

Fernández PA, Hurd CL, Roleda MY. 2014. Bicarbonate uptake via an anion exchange protein is the main mechanism of inorganic carbon acquisition by the giant kelp *Macrocystis pyrifera* (Laminariales, Phaeophyceae) under variable pH. Journal of Phycology **50,** 998–1008.

Fernández PA, Roleda MY, Rautenberger R, Hurd CL. 2018. Carbonic anhydrase activity in seaweeds: overview and recommendations for measuring activity with an electrometric method, using *Macrocystis pyrifera* as a model species. Marine Biology **165,** 88.

Fujiwara S, Fukuzawa H, Tachiki A, Miyachi S. 1990. Structure and differential expression of 2 genes encoding carbonic-anhydrase in *Chlamydomonas reinhardtii*. Proceedings of the National Academy of Sciences USA **87,** 9779–9783.

Giordano M, Beardall J, Raven JA. 2005. CO_2 concentrating mechanisms in algae: mechanisms, environmental modulation, and evolution. Annual Review of Plant Biology **56,** 99–131.

Granbom M, Pedersén M. 1999. Carbon acquisition strategies of the red alga *Eucheuma denticulatum*. Hydrobiologia **398/399,** 349–354.

Gravot A, Dittami SM, Rousvoal S, Lugan R, Eggert A, Collen J, Boyen C, Bouchereau A, Tonon T. 2010. Diurnal oscillations of metabolite abundances and gene analysis provide new insights into central metabolic processes of the brown alga *Ectocarpus siliculosus*. New Phytologist **188,** 98–110.

Hackl T, Hedrich R, Schultz J, Förster F. 2014. Proovread: large-scale high-accuracy pacbio correction through iterative short read consensus. Bioinformatics **30,** 3004–3011.

Han SJ, Maberly SC, Gontero B, Xing ZF, Li W, Jiang HS, Huang WM. 2020. Structural basis for C4 photosynthesis without Kranz anatomy in leaves of the submerged freshwater plant *Ottelia alismoides.* Annals of Botany doi: https://doi.org/ 10.1093/aob/mcaa005

Harada H, Matsuda Y. 2005. Identification and characterization of a new carbonic

anhydrase in the marine diatom *Phaeodactylum tricornutum*. Canadian Journal of Botany **83,** 909–916.

Harada H, Nakatsuma D, Ishida M, Matsuda Y. 2005. Regulation of the expression of intracellular β-carbonic anhydrase in response to CO_2 and light in the marine diatom *Phaeodactylum tricornutum.* Plant Physiology **139,** 1041–1050.

Huang WM, Shao H, Zhou SN, Zhou Q, Fu WL, Zhang T, Jiang HS, Li W, Gontero B, Maberly SC. 2018. Different CO_2 acclimation strategies in juvenile and mature leaves of *Ottelia alismoides*. Photosynthesis Research **138,** 219–232.

Iversen LL, Winkel A, Baastrup-Spohr L, Hinke AB, Alahuhta J, Baatrup-Pedersen A, Birk S, Brodersen P, Chambers PA, Ecke F, Feldmann T, Gebler D, Heino J, Jespersen TS, Moe SJ, Riis T, Sass L, Vestergaard O, Maberly SC, Sand-Jensen K, Pedersen O. 2019. Catchment properties and the photosynthetic trait composition of freshwater plant communities. Science **366,** 878–881.

James PL, Larkum AWD. 1996. Photosynthetic inorganic carbon acquisition of *Posidonia australis*. Aquatic Botany **55,** 149–157.

Jensen EL, Clement R, Kosta A, Maberly SC, Gontero B. 2019. A new widespread subclass of carbonic anhydrase in marine phytoplankton. The ISME Journal **13,** 2094–2106.

Karlsson J, Clarke AK, Chen ZY, Hugghins SY, Park YI, Husic HD, Moroney JV, Samuelsson G. 1998. A novel alpha-type carbonic anhydrase associated with the thylakoid membrane in *Chlamydomonas reinhardtii* is required for growth at ambient CO_2. EMBO Journal **17,** 1208–1216.

Klavsen SK, Madsen TV, Maberly SC. 2011. Crassulacean acid metabolism in the context of other carbon-concentrating mechanisms in freshwater plants: a review. Photosynthesis Research **109,** 269–279.

Klenell M, Snoeijs P, Pedersén M. 2004. Active carbon uptake in *Laminaria digitata* and *L. saccharina* (Phaeophyta) is driven by a proton pump in the plasma membrane. Hydrobiologia **514,** 41–53.

Larsson C, Axelsson L. 1999. Bicarbonate uptake and utilization in marine macroalgae. European Journal of Phycology **34,** 79–86.

Maberly SC, Spence DHN. 1983. Photosynthetic inorganic carbon use by freshwater plants. Journal of Ecology **71,** 705–724.

Maberly SC. 1990. Exogenous sources of inorganic carbon for photosynthesis by

marine macroalgae. Journal of Phycology **26,** 439–449.

Maberly SC. 1996. Diel, episodic and seasonal changes in pH and concentrations of inorganic carbon in a productive lake. Freshwater Biology **35,** 579–598.

Maberly SC, Madsen TV. 1998. Affinity for CO_2 in relation to the ability of freshwater macrophytes to use HCO_3. Functional Ecology **12,** 99–106.

Maberly SC, Gontero B. 2017. Ecological imperatives for aquatic CO_2-concentrating mechanisms. Journal of Experimental Botany **68,** 3797–3814.

Maberly SC, Gontero B. 2018. Trade-offs and synergies in the structural and functional characteristics of leaves photosynthesizing in aquatic environments. In: Adams III WW, Terashima I. (eds.) The leaf: a platform for performing photosynthesis. Advances in photosynthesis and respiration (Including bioenergy and related processes). Springer, Cham. 307–343.

Millhouse J, Strother S. 1986. Salt-stimulated bicarbonate-dependent photosynthesis in the marine angiosperm *Zostera muelleri*. Journal of Experimental Botany **37,** 965–976.

Moroney JV, Husic HD, Tolbert NE. 1985. Effect of carbonic anhydrase inhibitors on inorganic carbon accumulation by *Chlamydomonas reinhardtii*. Plant Physiology **79,** 177–183.

Moroney JV, Chen ZY. 1998. The role of the chloroplast in inorganic carbon uptake by eukaryotic algae. Canadian Journal of Botany **76,** 1025–1034.

Moroney JV, Bartlett SG, Samuelsson G. 2001. Carbonic anhydrases in plants and algae. Plant Cell & Environment **24,** 141–153.

Moroney JV, Ma Y, Frey WD, Fusilier KA, Pham TT, Simms TA, DiMario RJ, Yang J, Mukherjee B. 2011. The carbonic anhydrase isoforms of *Chlamydomonas reinhardtii*: intracellular location, expression, and physiological roles. Photosynthesis Research **109,** 133–149.

Nakajima K, Tanaka A, Matsuda Y. 2013. SLC4 family transporters in a marine diatom directly pump bicarbonate from seawater. Proceedings of the National Academy of Sciences USA **110,** 1767–1772.

Poliner E, Panchy N, Newton L, Wu G, Lapinsky A, Bullard B, Zienkiewicz A, Benning C, Shiu SH, Farré EM. 2015. Transcriptional coordination of physiological responses in *Nannochloropsis oceanica* CCM1779 under light/dark cycles. Plant Journal **83,** 1097–1113.

Prins HBA, Snel JFH, Helder RJ, Zanstra PE. 1980. Photosynthetic HCO_3^- utilization and OH^- excretion in aquatic angiosperms: light induced pH changes at the leaf surface. Plant Physiology **66,** 818–822.

Raven JA. 1970. Exogenous inorganic carbon sources in plant photosynthesis. Biological Reviews **45,** 167–221.

Roberts RJ, Carneiro MO, Schatz MC. 2013. The advantages of SMRT sequencing. Genome Biology **14,** 405.

Romero MF, Chen AP, Parker MD, Boron WF. 2013. The SLC4 family of bicarbonate (HCO_3^-) transporters. Molecular Aspects of Medicine **34,** 159–182.

Samukawa M, Shen C, Hopkinson BM, Matsuda Y. 2014. Localization of putative carbonic anhydrases in the marine diatom, *Thalassiosira pseudonana*. Photosynthsis Research **121,** 235–249.

Satoh D, Hiraoka Y, Colman B, Matsuda Y. 2001. Physiological and molecular biological characterization of intracellular carbonic anhydrase from the marine diatom *Phaeodactylum tricornutum.* Plant Physiology **126,** 1459–1470.

Shao H, Gontero B, Maberly SC, Jiang HS, Cao Y, Li W, Huang WM. 2017. Responses of *Ottelia alismoides*, an aquatic plant with three CCMs, to variable CO_2 and light. Journal of Experimental Botany **68,** 3985–3995.

Sharkia R, Beer S, Cabantchik ZI. 1994. A membrane-located polypeptide of *Ulva* sp. which may be involved in HCO_3^- uptake is recognized by antibodies raised against the human red-blood-cell anion-exchange protein. Planta **194,** 247–249.

Silva TSF, Melack JM, Novo EMLM. 2013. Responses of aquatic macrophyte cover and productivity to flooding variability on the Amazon floodplain. Global Change Biology **19,** 3379–3389.

Sowah D, Casey JR. 2011. An intramolecular transport metabolon: fusion of carbonic anhydrase II to the COOH terminus of the Cl^-/HCO_3^- exchanger, AE1. American Journal of Physiology-Cell Physiology **301,** C336–C346.

Staal M, Elzenga JTM, Prins HBA. 1989. ^{14}C fixation by leaves and leaf cell protoplasts of the submerged aquatic angiosperm *Potamogeton lucens:* carbon dioxide or bicarbonate? Plant Physiology **90,** 1035–1040.

Steemann-Nielsen E. 1947. Photosynthesis of aquatic plants with special reference to the carbon sources. Dansk Botanisk Arkiv Udgivet af Dansk Botanisk Forening **8,** 3–71.

Sterling D, Reithmeier RAF, Casey JR. 2001. A transport metabolon: Functional interaction of carbonic anhydrase II and chloride/bicarbonate exchangers. The Journal of Biological Chemistry **276,** 47886–47894.

Tachibana M, Allen AE, Kikutani S, Endo Y, Bowler C, Matsuda Y. 2011. Localization of putative carbonic anhydrases in two marine diatoms, *Phaeodactylum tricornutum* and *Thalassiosira pseudonana*. Photosynthesis Research **109,** 205–221.

Thornell IM, Bevensee MO. 2015. Regulators of *Slc4* bicarbonate transporter activity. Frontiers in Physiology **6,** 166.

Tsuji Y, Nakajima K, Matsuda Y. 2017. Molecular aspects of the biophysical CO_2-concentrating mechanism and its regulation in marine diatoms. Journal of Experimental Botany **68,** 3763–3772.

van Hille R, Fagan M, Bromfield L, Pott R. 2014. A modified pH drift assay for inorganic carbon accumulation and external carbonic anhydrase activity in microalgae. Journal of Applied Phycology **26,** 377–385.

Zhang YZ, Yin LY, Jiang HS, Li W, Gontero B, Maberly SC. 2014. Biochemical and biophysical CO_2 concentrating mechanisms in two species of freshwater macrophyte within the genus *Ottelia* (Hydrocharitaceae). Photosynthesis Research **121,** 285–297.

Zou DH, Gao KS. 2010. Acquisition of inorganic carbon by *Endarachne binghamiae* (Scytosiphonales, Phaeophyceae). European Journal of Phycology **45,** 117–126.

Figure legends

Figure 1. Example of a typical pH-drift over time (one replicate) for *O. alismoides* tested at an initial alkalinity of 1 mequiv L^{-1} without (control) or with inhibitors (AZ, DIDS).

Figure 2. Analysis of pH drift experiments without (control) or with inhibitors (AZ and DIDS) in *O. alismoides*. (A) Final pH; (B) Final CO_2 concentration; (C) Initial slope of Ci uptake rate *vs* concentration of CO_2 (between 15~40 μM), α_C; (D) CO_2 compensation point ($CP(CO_2)$); (E) C_T/Alk. Values represent means ± SE, n=3. Letters indicate statistical differences between control and treatments (one-way ANOVA, Duncan's and Tukey's post-hoc tests $P<0.05$).

Figure 3. Effect of AZ or DIDS on the Ci uptake rate at different CO_2 concentrations in *O. alismoides*. (A) Ci uptake rate; (B) Ci uptake inhibition. Values represent means ± SE, n=3. Letters in (A) indicate statistical differences among control and inhibitor treatments within CO_2 concentrations (one-way ANOVA, Duncan's and Tukey's post-hoc tests $P<0.05$). Letters and symbols in (B) indicate statistical differences among different CO_2 concentrations within inhibitor treatment (Mann–Whitney test $P<0.05$).

Figure 4. Effect of removal of AZ on Ci uptake rate in *O. alismoides* leaves at different CO_2 concentrations. Values represent means ± SE, n=3. (A) 0.1 mM AZ; (B) 0.2 mM AZ. The inhibitor was removed by washing the treated leaves in the post-control (see Methods). Letters indicate statistical differences between the control and inhibitor treatments of AZ for each CO_2 concentration (one-way ANOVA, Duncan's and Tukey's post-hoc tests $P<0.05$).

Figure 5. Effect of AZ and DIDS on Ci uptake rate and external CA activity in leaves of *O. alismoides* acclimated to high CO_2 (HC) or low CO_2 (LC) and measured at an initial CO_2 concentration of 12 μM. (A) Ci uptake rate; (B) Inhibition of Ci uptake rate;

(C) External CA activity and (D) Inhibition of external CA activity. Values represent means ± SE, n=3. For panels (A) and (C), letters indicate statistical differences between the control and different treatments at HC and LC acclimated leaves using one-way ANOVA, Duncan's and Tukey's post-hoc tests $P<0.05$. For panels (B) and (D), uppercase and lowercase letters indicate statistical differences among inhibitor treatments at HC and LC respectively using the Mann–Whitney test $P<0.05$; the line above the two columns indicates the statistical differences between HC and LC treatments (Mann–Whitney test $P<0.05$).

Figure 6. Phylogenetic tree of αCA-1 isoforms, prediction of location for αCA-1 peptides, and mRNA expression for αCA-1 and SLC4 HCO_3^- transporters in *O. alismoides* leaves acclimated at high CO_2 (HC) and low CO_2 (LC) concentrations. (A) Phylogenetic tree of αCA-1 isoforms in *O. alismoides*; (B) Output of the predicted location tested on the four isoforms for putative αCA-1 from the Target P server; (C) mRNA expression for αCA-1; (D) mRNA expression for SLC4 HCO_3^- transporters. In panel (A), the scale bar at the bottom represents the evolutionary distances in amino acid sequences. In panel (B), cTP is the chloroplast transit peptide, mTP is the mitochondrial targeting peptide, SP is the secretory pathway, Other stands for other locations, Loc gives the final prediction, RC is the reliability class (from 1 to 5), where 1 indicates the strongest prediction. The default was used to choose cutoffs for the predictions. Values in panels (C) and (D) represent the mean ± SE, n=3. Data of SLC4 HCO_3^- transporters expression in panel (D) correspond to the highest expressed transcript. The lines in panels (C) and (D) above the two columns indicate the statistical differences between LC and HC treatment (one-way ANOVA, $P<0.05$).

Figure 7. A model of inorganic carbon acquisition in *O. alismoides*. (A) Model structure. ① passive diffusion of CO_2; ② diffusion of HCO_3^- and conversion to CO_2 by αCA-1 at the plasmalemma; ③ diffusion of HCO_3^- and transfer across the plasmalemma by SLC4 HCO_3^- transporters. (B) The contribution of CO_2-diffusion, diffusion of HCO_3^-

and conversion to CO_2 via αCA-1 and transfer of HCO_3^- by SLC4 HCO_3^- transporters to total Ci uptake at different CO_2 concentrations.

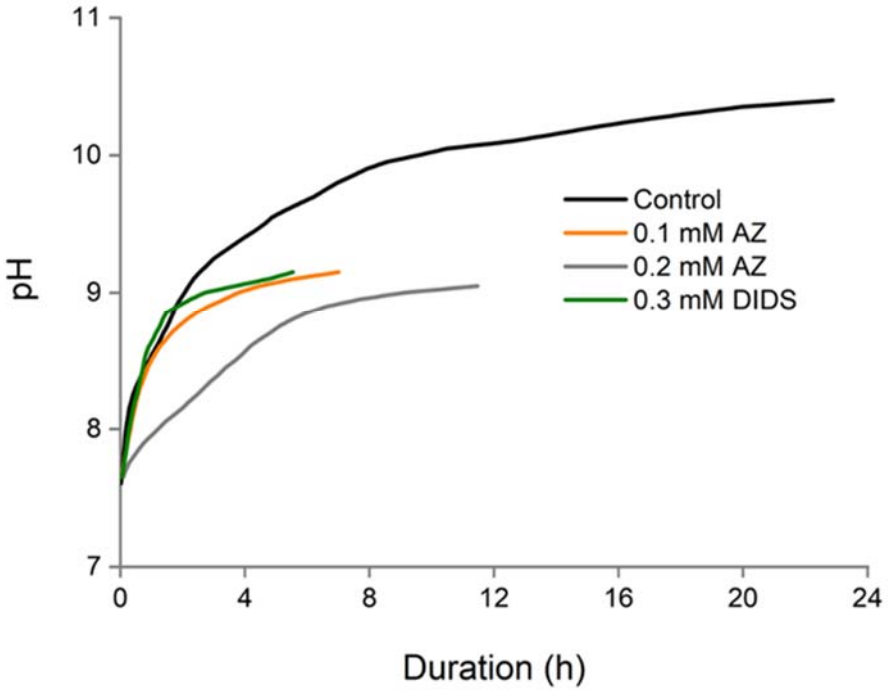
11
10
9
8
7
pH
0
4
8
12
16
20
24
Duration (h)
Control
0.1 mM AZ
0.2 mM AZ
0.3 mM DIDS

Figure 1

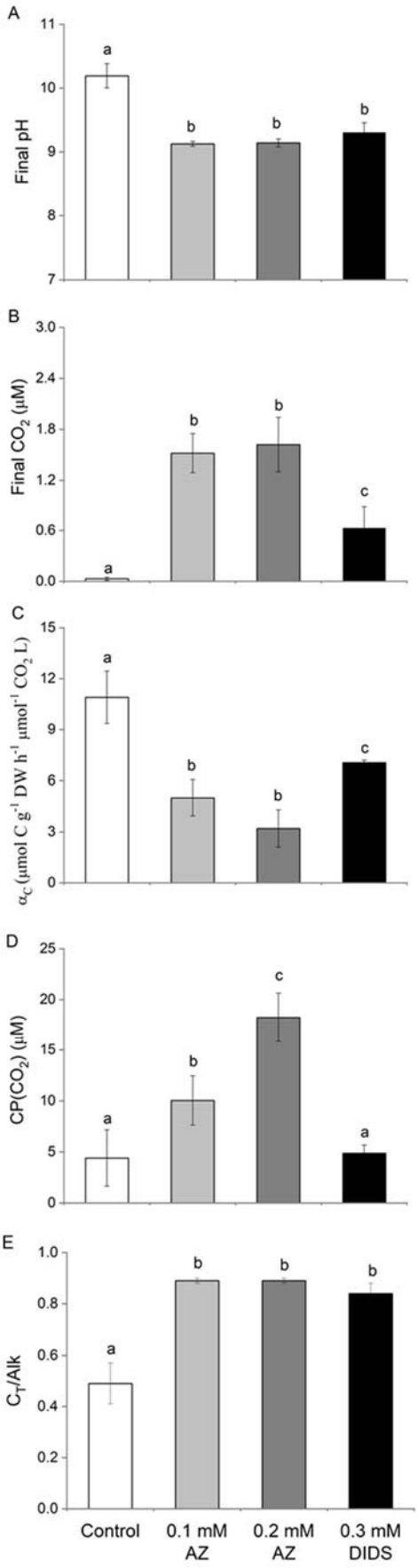
A
Final pH
11
10
9
8
7
a
b
b
b
B
Final CO_2 (μM)
3.0
2.4
1.8
1.2
0.6
0.0
a
b
b
c
C
α_C (μmol C g^{-1} DW h^{-1} μmol^{-1} CO_2 L)
15
12
9
6
3
0
a
b
b
c
D
CP(CO_2) (μM)
25
20
15
10
5
0
a
b
c
a
E
C_T/Alk
1.0
0.8
0.6
0.4
0.2
0.0
a
b
b
b
Control
0.1 mM AZ
0.2 mM AZ
0.3 mM DIDS

Figure 2

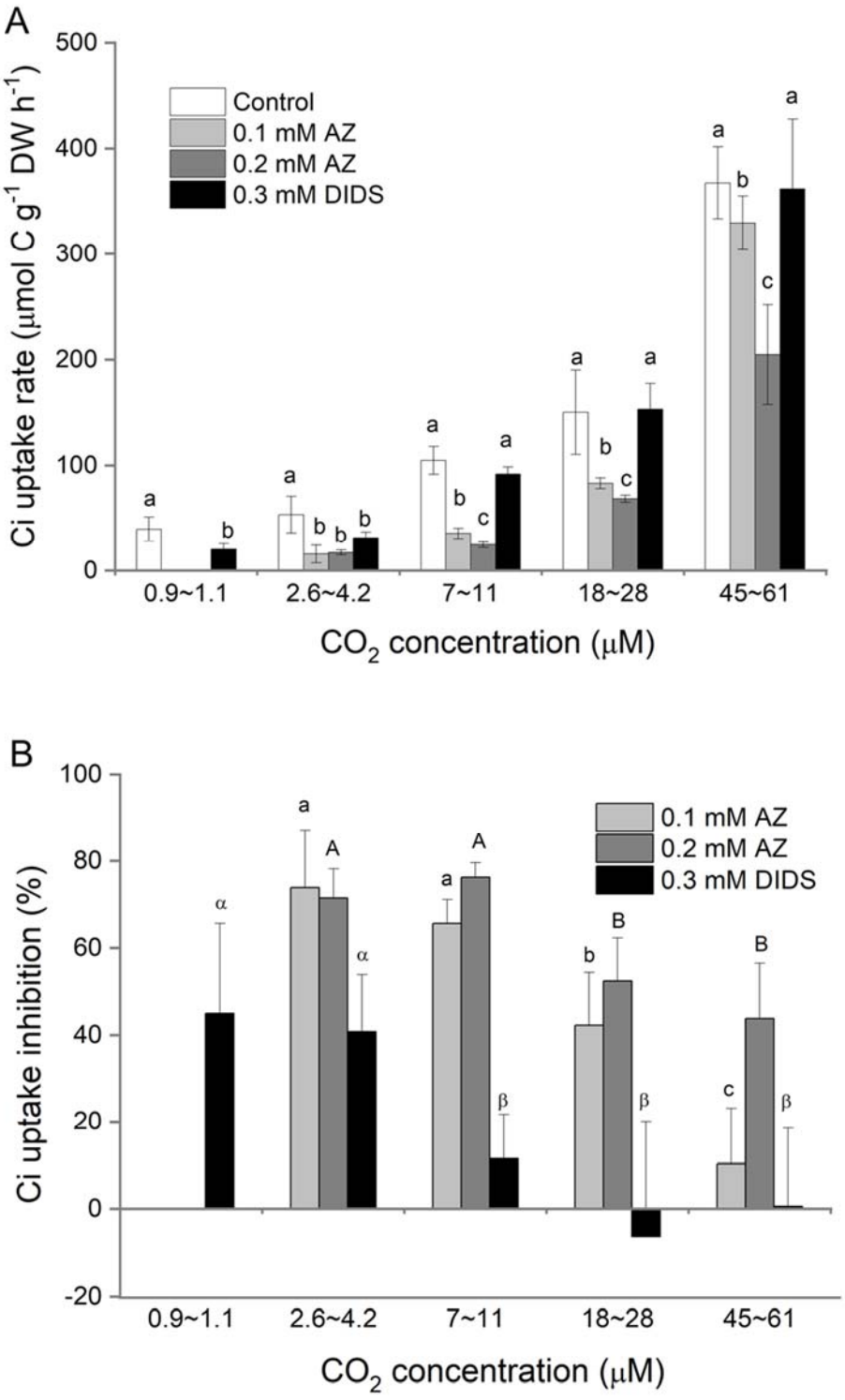
A
Ci uptake rate (μmol C g-1 DW h-1)
Control
0.1 mM AZ
0.2 mM AZ
0.3 mM DIDS
0.9~1.1
2.6~4.2
7~11
18~28
45~61
CO2 concentration (μM)
B
Ci uptake inhibition (%)
0.1 mM AZ
0.2 mM AZ
0.3 mM DIDS
0.9~1.1
2.6~4.2
7~11
18~28
45~61
CO2 concentration (μM)

Figure 3

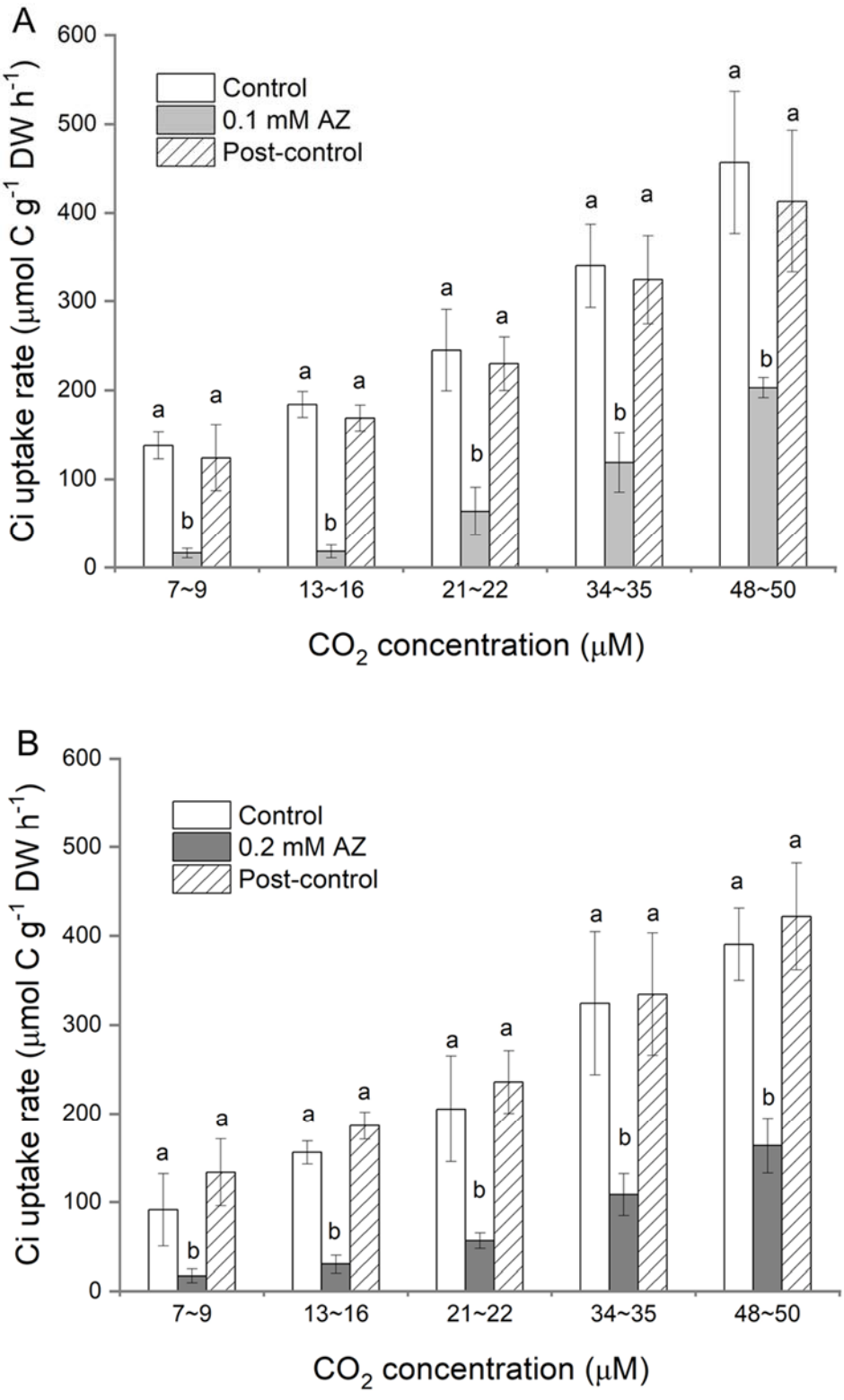
A
Ci uptake rate (μmol C g-1 DW h-1)
Control
0.1 mM AZ
Post-control
CO2 concentration (μM)
7~9
13~16
21~22
34~35
48~50
B
Ci uptake rate (μmol C g-1 DW h-1)
Control
0.2 mM AZ
Post-control
CO2 concentration (μM)

Figure 4

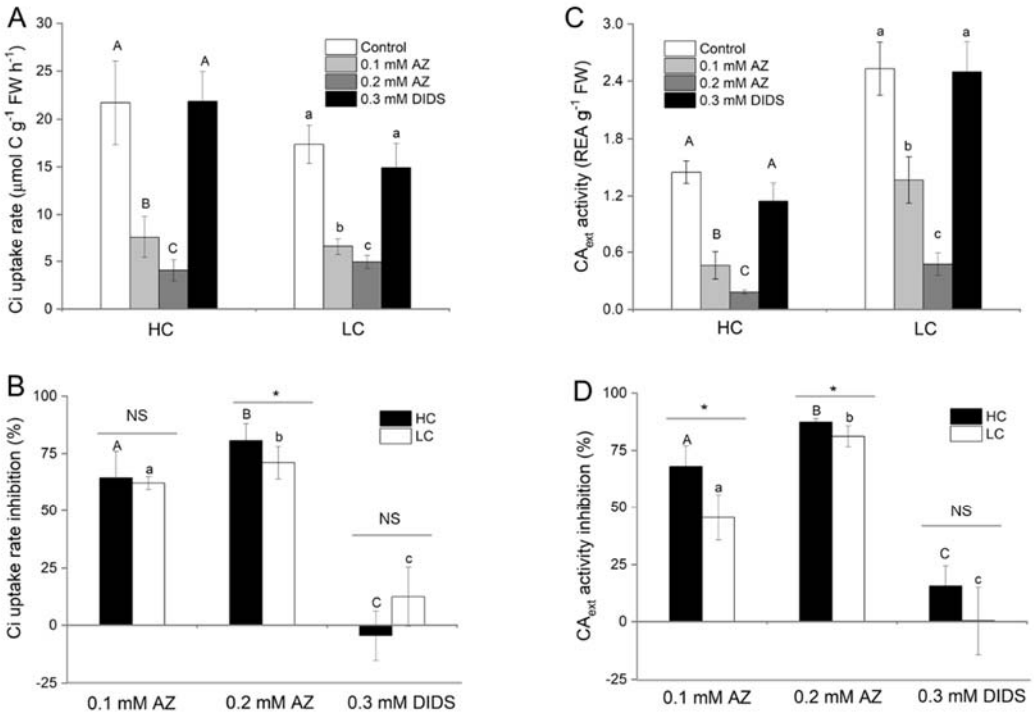
A
Ci uptake rate (μmol C g-1 FW h-1)
Control
0.1 mM AZ
0.2 mM AZ
0.3 mM DIDS
HC
LC
C
CAext activity (REA g-1 FW)
B
Ci uptake rate inhibition (%)
NS
*
0.1 mM AZ
0.2 mM AZ
0.3 mM DIDS
D
CAext activity inhibition (%)

Figure 5

A

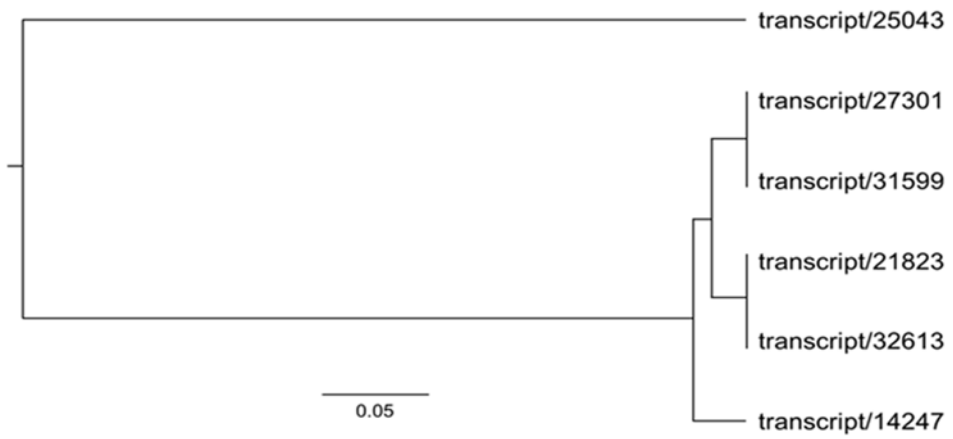

B

Putative protein	Isoforms	cTP	mTP	SP	Other	Loc	RC
αCA-1	1	0.077	0.025	0.885	0.013	SP	1
αCA-1	2	0.023	0.023	0.951	0.050	SP	1
αCA-1	3	0.021	0.025	0.952	0.054	SP	1
αCA-1	4	0.023	0.023	0.951	0.050	SP	1

C

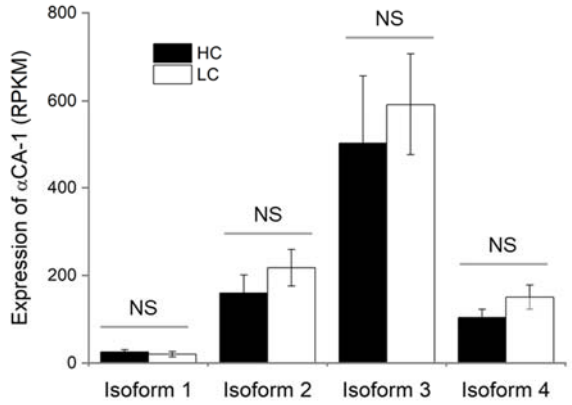

D

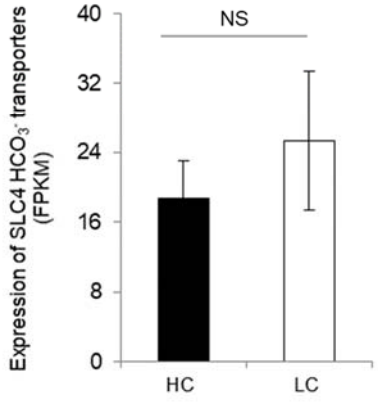

Figure 6

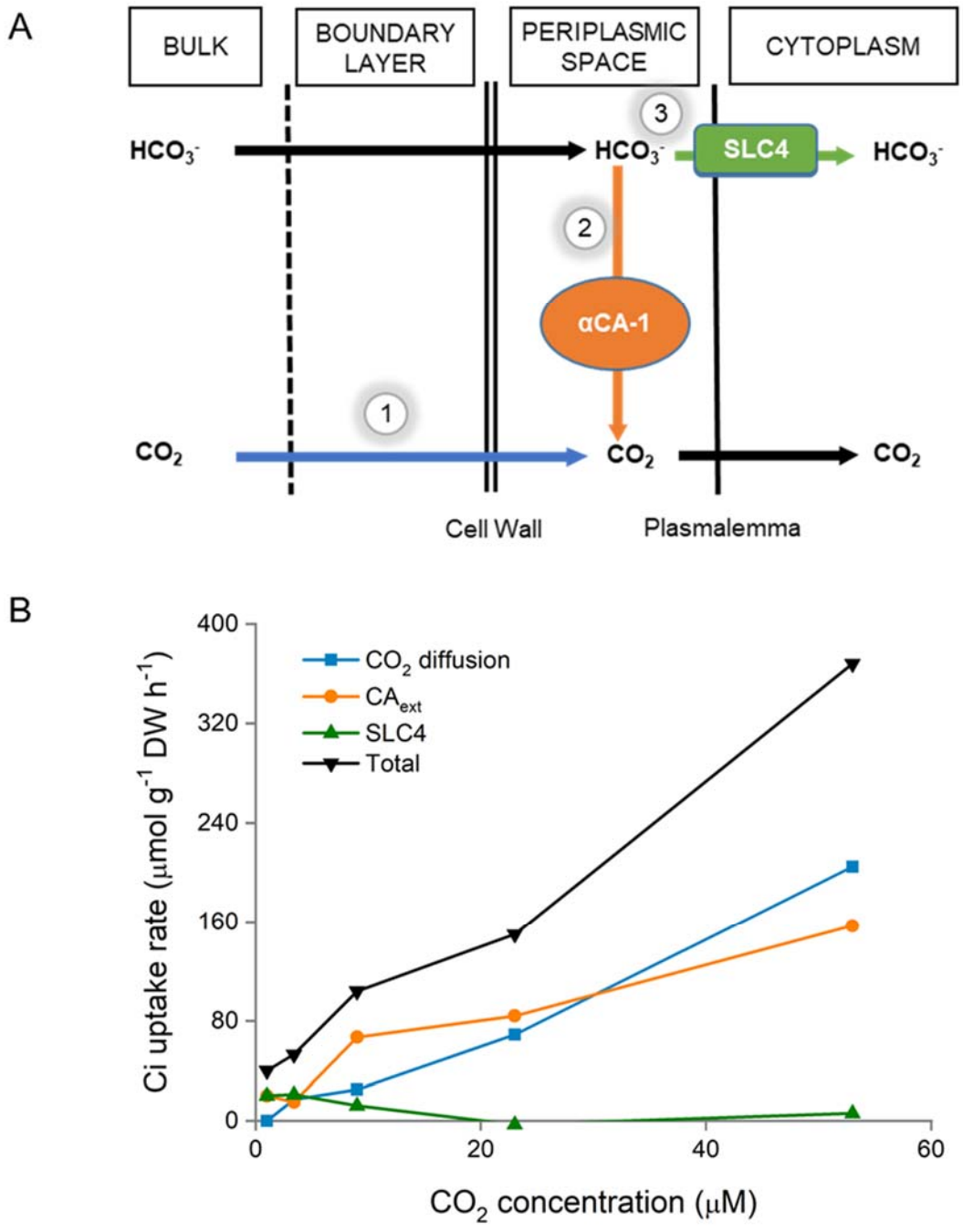
A
BULK
BOUNDARY LAYER
PERIPLASMIC SPACE
CYTOPLASM
HCO3-
HCO3-
SLC4
HCO3-
3
2
αCA-1
1
CO2
CO2
CO2
Cell Wall
Plasmalemma
B
CO2 diffusion
CAext
SLC4
Total
Ci uptake rate (μmol g-1 DW h-1)
400
320
240
160
80
0
0
20
40
60
CO2 concentration (μM)

Figure 7